Fibre-Reinforced Glass/Silicate Composites: Effect of Fibrous Reinforcement on Intumescence Behaviour of Silicate Matrices as a Fire Barrier Application

B.K. Kandola*, M.H. Akonda, A.R. Horrocks

Institute for Materials Research and Innovation, University of Bolton, Deane Road, Bolton, BL3 5AB, UK

** Corresponding author. Tel.: +44 1 204 903517. E-mail address: B.Kandola@bolton.ac.uk*

Abstract

This paper is the third in series on fire-resistant laminated glass composites containing an intumescent silicate interlayer and studies the effect of reinforcing fibres on the intumescent behaviour of the silicate matrices. Two silicate matrices with different silica/metal oxide ratios (SiO_2:Na_2O) were reinforced by polypropylene (PP), polyamide 66 (PA66), AR-glass (ARG) and stainless steel (ST) fibres, selected because of their alkali and UVA resistant properties. Thermal degradative behaviour of fibre/silicate mixtures having 5/95 and 10/100 mass ratios were examined to understand the effect of each fibre type on the intumescence of each silicate. Fibre reinforcements of the silicate layer were either as a nonwoven web or as a woven mesh. The intumescent properties of silicates were studied by heating the composites in a furnace at 450^{o}C for five minutes and measuring the intumescent layer thickness. The results showed that all fibre types in nonwoven web reinforcements had a negative effect while inorganic glass fibre in a woven mesh form had a negligible effect on the overall intumescence of silicate matrices. It was proposed that while fibre type was of minor importance, the fabric structure played an

important role in inhibiting intumescence. Preferred reinforcement should preferably have open mesh-like characteristics.

Key words: Silicate matrix, Intumescent, Fire-resistance, Fibre-reinforcement, Glass composites

1. Introduction

It is well known that glass is not combustible but on exposures to high temperatures or fire, a monolithic glass pane cracks and cannot act as an effective barrier for advancing fire and smoke to spread in adjoining compartments of a building or a ship, for example. For such applications where fire safety regulations require the use of fire barriers, fire-rated glass products capable of offering varying degree of protection ranging from 20 min to 3 h according to BS476 Part 22, are used [1,2]. The fire-rated glass acts as a passive fire protection, restricting the fire damage to a limited area.

Out of many types of fire-rated glass developed over last three decades [3-5], the most successful and widely used is a multi-layered laminated glass, where a soluble alkali-metal silicate as an intumescent interlayer is sandwiched between two glass sheets [5]. The silicate interlayer intumesces on exposure to fire, providing a degree of fire protection for a period of time. The intumescence of the alkali-metal silicate internal layer results from rapid liberation of water vapour on exposure to high temperatures. Water-soluble sodium silicate is obtained by reacting silica with sodium or potassium carbonate [6,7] or bicarbonate, maintaining SiO_2:Na_2O molar

ratios (R) from 1.6 to 3.9. As the ratio R (SiO_2/Na_2O) increases, pH value decreases [7]. Dilution of solutions decreases the pH and high molecular mass particles are formed due to rapid polymerization and simultaneous aggregation. For greater aggregation, higher R values (> 3.5) are preferred [8].

Intumescent soluble silicates consist of water in free and bound forms [9]. The bound water may be (i) hydrogen-bonded to surface silanol group of polysilicate ions, (ii) as ionic hydration, where water molecules are associated with cations and polysilicate ions, and (iii) structural water present as SiOH groups on polysilicate ions [10,11]. Free water and water hydrogen-bonded to silanol groups are released at low (<130^oC) or even at room temperatures [11]. On the other hand, ionically hydrated water is released in the temperature range 130-200^oC, where its rapid evolution generates intumescence. Structural water is released at comparatively high temperatures, ranging from 200-500^oC while the polysilicate elements begin to cross-link by condensation of SiOH groups to form –Si–O–Si bonds. At approximately 900^oC the sodium silicate starts to melt to form sodium silicate glass. The overall intumescence property and solubility of silicates depends on the strength of cationic cross-links between adjacent polysilicate particles. Degrees of solubility and intumescence both decrease in the order K^+ >Na^+>Li^+ i.e., the smaller the cationic atom, the lower the degrees of intumescence and solubility [11]. Thus ionic hydration is the primary mechanism for the water absorption of the silicate samples.

The SiO_2:M_2O molar ratio also affects the dehydration and intumescence of soluble silicates [12], for which a lower ratio is more favourable. If the SiO_2:M_2O ratio is increased i.e. pH value

is reduced, the polysilicate particles size increases, the surface charge density decreases and the solution becomes more colloidal. Such solutions have a higher probability of forming –Si–O–Si– bond between particles as the solution dries thus providing greater water resistance and a decrease in the intumescence property [12]. During initial fire exposure, the intumescent interlayer absorbs heat and when the interlayer reaches the required temperature, the residual water in the interlayer evaporates consequently consuming a major part of the energy released by the incident fire radiant energy. Concurrently, the interlayer expands generating a thick, tough insulating shield and hard foam, which works as a protection against smoke and flame penetration. Such glass-silicate-glass composites when exposed to fire, can produce a degree of fire protection for considerable period of time, but have limited impact resistance [13].

In our previous publications we have explored the use of some alkali-resistant fibres [14,15] as a reinforcement to increase the impact resistance of laminated glass-silicate-glass composites, which are commercially used as fire-rated glass products [5]. The results indicated that certain fibres such as polypropylene, polyamide 66, alkali resistant glass and steel fibres could significantly enhance their impact performance [15], although transparency of the matrices sandwiched between glass sheets can be affected, depending upon the reinforcement type. In this paper the effect of these reinforcing fibres on the intumescent behaviour of the silicate matrices within glass composites under thermal shock is studied. To best of our knowledge such a systematic study has not been carried out before.

2. Experimental Details

2.1. Materials

2.1.1. Intumescent silicate matrices

Two types of water-soluble sodium silicate matrices, PS-A and PS-B were sourced from Pilkington plc (UK). These silicate solutions contain silica and sodium oxide at different molar ratios with pH 11.8 and 13.6, respectively. Their compositions are reported in Table 1.

2.1.2. Fibres

These have been fully described in our previous publications [14,15] and are summarized below and in Table 2:

(1) Polypropylene (PP): Nonwoven web of area density, prepared from UV stable PP fibres (Fibre Vision, Denmark) using an Automatex laboratory nonwoven line.

(2) Polyamide 66 (PA66): Nonwoven web of area density 19 g/m^2 from PA66 fibres (DuPont, USA), produced similarly to PP.

(3) Alkali resistant glass (ARG) fibre: Two types of reinforcements were used; nonwoven veil (ARGV) of 44 g/m^2, woven mesh (ARGM) from continuous filaments (0.8 mesh/cm) of 88 g/m^2), both sourced from Nippon Glass, Japan.

(4) Steel (ST): Woven mesh from continuous stainless steel filaments (12 mesh/cm); 40 g/m^2), sourced from TWP Inc, USA.

2.2. Sample preparation

2.2.1. Silicate-fibre mixtures for thermal analysis

Mixtures of pulverized silicate matrices and fibres were used for thermal analytical studies. Dry silicate matrices were pulverized using a pestle and mortar yielding particle sizes <1 μm . PA 66,

PP and ARGV fibres were pulverized also yielding particle sizes <1 μm by using a Wiley mill with a 1 mm screen. Then pulverized matrices were mixed properly with 5 and 10% (by mass) of pulverized fibres and samples are referred to as PS-A+5%F and PS-B+5%F (Tables 3 and 4), where F=PP, PA66 or ARG. The steel fibre was not used in this study as it was difficult to pulverize the fibres in the lab.

2.2.2. Glass-silicate-glass composite laminates

To prepare fibre-reinforced silicate layered glass composites, a fixed amount of nonwoven web or mesh (125x125 mm) was placed on a 3 mm thick silicate glass sheet (bottom layer of composite) with a silicon side barrier (10 mm height) fitted. The fibre content was selected based on our previous work to provide optimized mechanical properties and the transparency to these composites [15]. Then a fixed amount of silicate solution was poured very slowly over the web or mesh and the whole assembly was transferred to an oven and dried at 100^{o}C for 14-16 h to create 1.7±0.2 mm thick silicate layer. The side barriers were cut away and another 3 mm thick glass sheet was placed on top of the dry glass/silicate sheet. A small amount of glycerol was used to wet the dry silicate surface before lowering this second glass sheet and whole assembly was further dried for 12 h at 90^{o}C under a load of 10 kg/m^2 to make sandwich-type, laminated glass-silicate-glass and glass-silicate/fiber-glass composite structures (see Figure 1(a)). The details of the composite samples are given in Table 2, in which samples are referred to as PS –A/B + FR, where FR = fibre reinforcement, e.g., PP, PA66, ARGV, ARGM and ST.

2.3. Thermal stability and intumescence performance evaluation

2.3.1. Thermal analysis

For simultaneous DTA/TGA analysis, a TA Instrument STD2606 was used under flowing nitrogen (100ml/min) at a heating rate of 10^{o}C min^{-1}. Sample mass of 10±0.5 mg was used every time.

2.3.2. Intumescence performance of laminated composites

This was determined in terms of the change of silicate layer thickness and resulting foam density using a thermal shock method [16], where composite specimens (100 mm x 100 mm) were placed in a Carbolite furnace at 450^{o}C for 5 minutes. The intumescent behaviour was determined using equation (1) as the expansion of the silicate layer in each composite as shown in Figures 1(b) and (c) and defined as:

$$Degree\ of\ Intumescence\ (DI) = \frac{T_2 - T_1}{T_1} \qquad (1)$$

where, T_1 and T_2 are the thicknesses in mm of the interlayer in the composite specimens before and after thermal shock as shown by digital images of the samples before and after the test (see Figures 1(a) and (b) and (c) respectively).

The density of intumescent layer or foam density was calculated using equation (2) [16]:

$$Foam\ Density\ (g/cm^3) = \frac{Mass\ of\ silicate\ (g)}{Volume\ of\ the\ foam\ (cm^3)} \qquad (2)$$

where, the mass of silicate = (total sample mass – mass of two laminated glass sheets) and the volume of foam = composite length x composite width x thickness of the interlayer (T_2)

2.3.3. Scanning electron microscopy

A Cambridge S-200 scanning electron microscope (Deben, UK Ltd.) was used to study the morphology of the charred structure, obtained after subjecting composite specimens to 450 ^{o}C for 5 min in a Carbolite furnace. Small amounts of charred interlayer samples specimens were mounted on stubs using double-sided sticking tape. The chamber pressure was kept at 0.2 mbr and the incident beam voltage was 5 kV.

3. Results and discussion

3.1. Thermal analytical studies

3.1.1. Intumescent silicate matrices

The DTA and TGA-DTG for the silicate samples alone and their mixtures with fibres are shown in Figures 2 and 3. Results obtained from the analysis of curves are given in Tables 3 and 4. As discussed before, the soluble silicates contain free and bound water. On heating, the release of water causes intumescence and the expanded char then acts as a thermal barrier for the underlying glass sheet [9-11]. The DTA peaks of the PS-A matrix in Figure 2(a) show that that there are two endothermic peaks at 100 and 146^{o}C followed by an exothermic peak at 352^{o}C (Table 3). The first endothermic peak is attributed to the loss of free water and water hydrogen-bonded to silanol groups [12,17]. The second DTA endothermic peak at 146^{o}C is due to ionically hydrated water released from the sodium silicate system. The exothermic peak at 352^{o}C

represents the release of structural water and joining of polysilicates by condensation of SiOH groups to form –Si–O–Si– groups [6,17]. The endothermic peak with maximum at about 590 ^{o}C is present in all PS-A samples (see Figure 2(a)) and so is probably due to silicate matrix only although no similar transition is observed in the PS-B samples in Figure 2(d). No mass loss is observed in Figure 2(b) at this temperature and so the transition is either a solid phase transition or a baseline effect. The intensity of the endotherm reduces in the presence of each fibre at 5% level (see below) and so this would suggest that the transition is not directly related to a silicate transition but could be a baseline effect caused by a sample geometric change peculiar to this silicate matrix. On the other hand in the PS-B silicate sample (see Figure 2(d)) the first endothermic peak is at a lower temperature (66^{o}C) than that of PS-A, representing easier loss of free water in the former. The second DTA endothermic peak observed at 146^{o}C in PS-A is absent in PS-B silicate, whereas the exothermic peak observed at 352^{o}C due to the release of structural water is at a similar temperature to that in PS-A silicate.

The TGA-DTG curves in Figures 2(b) and (e) indicate that both silicate samples have followed four steps of decomposition, as indicated by the stepwise mass changes between 40-120, 120-330, 330-420 and 420-540^{o}C, supported by a respective DTG peak for each stage (see Figures 2(c) and (d)). For direct comparison of both silicate samples, their mass (TGA) and derivative mass (DTG) values as a function of temperature are plotted in Figure 3(a). The first mass loss is due to release of free water indicated by the DTG peak at 104^{o}C (Table 3) in both samples, while the second mass loss (120-330^{o}C) is due to release of ionically bonded water, shown by the DTG peak at 140^{o}C in PS-A and 190^{o}C in PS-B, which is related to the intumescence performance of the dry silicate samples [17]. The third mass loss between 330-420^{o}C is attributed to dehydration

of polysilicate silanol groups to siloxane with the release of structural water showing as respective DTG peaks at 361^{o}C for both silicates. Finally, the mass loss >420 ^{o}C, with DTG peak at 506^{o}C in both silicates is due to decomposition of silicate [17,18]. As can be seen from the above discussion, both samples behave similarly except in the temperature range 120 - 330 ^{o}C, where mass loss is lower in PS-B, with a DTG peak at the higher temperature of 190 ^{o}C compared to PS-A. Expansion of the axes over this temperature range in Figure 3(b) clarifies this more, where this stage is designated 'A-B' where initial mass losses up to 120 ^{o}C are respectively 7.0 and 8.6% for PS-A silicate and PS-B, and 17.4 and 12.0 % in the temperature range 120 - 330 ^{o}C. The two silicates behave differently in this stage due to different SiO_2:Na_2O ratios and the rapid evolution of water vapour in this stage is responsible for their intumescent property. The mass loss over the 120-330^{o}C (A-B) range in PS-A (17.4%) indicates its higher degree of intumescence compared to PS-B (12.0% mass loss) silicate sample.

3.1.2. Silicate-fibre (PA66, PP, ARG) mixture thermal transitions

The thermal analytical behaviour of all fibres has been discussed in detail in our previous publication [14] and is summarized here in order to predict their effect on intumescence of the silicates. The DTA of PP showed two endothermic peaks with maxima at 163 and 461 ^{o}C (included in Table 3), representing melting and depolymerisation and/or decomposition of the polymer [14]. The TGA curve of PP indicated only 2.4% mass loss up to 330^{o}C (included in Table 4) above which degradation starts is completed by ~500^{o}C, with maximum mass loss at 460^{o}C as indicated by the DTG peak maximum [14]. At the temperature range of interest for intumescence to occur in silicates (120-330^{o}C), PP does not decompose, hence should not

interfere in the process. The fibre though will melt and may change the viscosity of the liquefying silicate.

For PA66 there were two endothermic DTA peaks observed at 261 and 430^{o}C, representing melting and decomposition of the polymer, respectively [14]. Thermogravimetric decomposition starts at 360^{o}C and is completed by ~485^{o}C with a maximum mass loss DTG peak at 448^{o}C and so like PP, PA66 should have minimal effect on the intumescence of silicates.

The DTA curve of AR-glass fibres showed no sharp peak as expected and only an exothermic base line shift was evident. No DTG peaks was observed, there was negligible (0.4%) mass loss up to 400^{0}C, which could be due to loss of size (typically at 0.5% by mass levels) from the fibre surfaces. This fibre should also not be expected to affect the intumescence of silicates.

The DTA, TGA and DTG curves for both matrices with 5% fibre contents are shown in Figure 2 and analysed results for 5 and 10% fibre mixtures are given in Table 3 as thermal transition temperatures and in Table 4 as TGA mass loss data. For PS-A/PP fiber mixtures (both 5 and 10%), the endothermic and exothermic peaks are at similar temperatures as for PS-A silicate alone with an extra endothermic peak at 462^{o}C (see Figure 2a and Table 3) due to the degradation of polypropylene fibre under nitrogen. There are five steps of mass loss, represented by five DTG peaks in Table 3 and the temperatures of mass loss steps are similar to those for the PS-A silicate alone (see Figure 2(b)) with an additional step represented by the DTG peak at 465^{o}C because of decomposition of the polypropylene. Similarly for the PS-A silicate-PA66 mixtures (5 and 10%), the two extra endothermic peaks at 255 (due to melting point of fibre) and 405^{o}C (due to decomposition of the fibre) are observed and other peaks (both endothermic and exothermic) are at the same temperatures as they are for the silicate matrix(see Figure 2(a) and

Table 3). In both PS-A silicate PP or PA66 mixtures, peaks observed in samples with 5 and 10% fibre are similar, but of higher intensities, representing decomposition of the respective fibres present. As temperatures approach 500^{o}C, respective PS-A sample DTA transitions and TGA mass loss transitions generally show some degree of correlation except for the addition of the DTA PA66 fusion endotherm in the PS-A-PA66 samples. Above 500^{o}C, the 506^{o}C DTG transitions in all PS-A-containing samples are not matched by obvious respective DTA peaks and the above-mentioned DTA endotherm at about 590^{o}C is not associated with any evident mass loss. Without further study here, we have no explanation for this transition.

Similar effects are seen for both PP and PA66 fibers in mixtures with PS-B, i.e., DTA and DTG responses and peak maxima observed for PS-B/PP and PS-B/PA66 mixtures are similar to the peaks reported for PS-B silicate alone (see Figure 2(d)), with any extra peaks being due to the respective fibre melting or decomposition transitions.

For silicate-ARG mixtures, the DTA curves in Figures 2(a) and 2(d) indicate that the endothermic and exothermic peaks maxima are at similar temperatures as for the respective silicates (see Table 3). In the PS-B/ARG fibre mixture, the endothermic peak at 167^{o}C is slightly more pronounced than for the silicate. Similarly, the DTG peak maxima for mixtures are also at similar temperatures as those for respective silicates (see Table 3). The ARG fibre contains 58-60% silica (SiO_2) [19], whereas the soluble silicates contain 28-31% silica (SiO_2) and this similarity in high silica content for both ARG fibre and silicates explains why the thermal behaviour of the silicates alone and silicate/ARG fibre mixtures are similar. The step-wise mass

losses are also similar for both silicate-ARG fibre mixtures in terms of their showing similar DTG peaks (Figures 2(b),(c),(e) and(f) and Table 3).

3.1.3. Effect of fibre presence on silicate mixture mass losses associated with intumescence

From TGA curves (with 5% fibres shown in Figures 2 and 3) step-wise actual sample mass losses were calculated and are presented in Table 4. In order to assess whether the presence of a given fibre in a silicate/fibre mixture influences the overall mass loss during a given degradation stage, the expected mass loss for each stage was calculated from the weighted average of individual TGA curves of each silicate and respective fibre present in the mixture. These calculated mass losses are presented in Table 4 as bracketed italicized values. Since for the intumescence process the temperatures of interest are up to 330^{o}C, the respective steps 40-120 and 120-330^{o}C are presented in Table 4. Mass loss values above 330 ^{o}C, i.e.330-600 ^{o}C, are also included so that total sample mass losses occurring throughout all three stages may be quantified. In the first step representing mass loss due to free water, presence of all fibres (PP, PA66 and ARG) at both 5 and 10% levels slightly increases the observed mixture mass loss (7-8%), compared to 7% for pure PS-A silicate and this difference, though small, is probably within experimental error and so may be considered to be negligible. These actual mass losses, however, are slightly higher than the calculated weighted averages of individual component mass loss values presented italicized in brackets. In the temperature range 120- 330 ^{o}C, where ionic water is liberated and the main intumescence occurs, the observed mass loss is 17.4% for PS-A silicate and the presence of each fibre decreases this to the range 13.9-14.8% at 5% and 13.6-15.4% with 10% fibre; these range values are now for each sample lower than the respective calculated averaged range values. While this suggests that the presence of fibre increases overall

mass loss over the 120-330°C range, the type of fibre has no obvious effect. This is not surprising as the DTA and DTG peak temperatures suggest no interaction between the PS-A matrix and any fibre present. Above 330 °C, the mass loss is increased with fibre presence from 7.7% for pure PS-A to ~15% with 5 or 10% PP and ~12-13% with 5 or 10% PA66 present, which represents decomposition of the respective fibres. For ARG fibre, there is minimal effect in this range as the glass fibre does not decompose. However, the calculated average mixture mass loss values do not bear a consistent relationship to respective actual values. Thus all former values for 5% fibre presence appear to be less than actual while 10% mixtures with PP or PA66 show greater values than actual and with ARG fibres no change.

In PS-B silicate/fibre mixtures the mass loss in the first step (RT-120 °C) is 7-8%, similar to that for PS-B (8.6%), within experimental error. In the temperature range 120-330 °C, the mass losses for all fibre mixtures are ~12%, the value for PS-B silicate alone, indicating no effect on water loss and hence intumescence. These actual values are also close to the expected calculated mass loss values although they are generally slightly less. This is different to the behavior of PS-A/fibre mixture samples, where actual mixture mass losses are reduced relative to the pure silicate and calculated mixture mass losses are generally slightly larger than respective actual values. Generally, however, it might be concluded that the presence of any fibre has a slightly negative effect on loss of water and hence intumescence. Above 330°C, and apart from the thermally stable ARG fibre, silicate-fibre mixture mass loss values are higher in PS-B/ PP and /PA66 fibre mixtures as a consequence of fibre degradation and calculated values are very similar to the respective actual mixture values (see Table 4).

Overall therefore, it may be concluded that based on DTA and TGA/DTG studies, this study shows that while the presence of each type of fibre has some effect on water liberation in PS-A silicate matrix, which is related to its intumecence property, the effect is minimal. In the PS-B matrix, however, any such effect is negligible. Hence, the selected fibres up to 10% content in the matrix should not have any significant detrimental effect on the observed intumescence of these matrices.

3.2. Intumescent performance of fiber-reinforced silicate interlayered composites

Fire performance of all composites samples in terms of their intumescence behavior has been studied by measuring the expansion of the silicate layer under thermal shock. Commercially fire resistance of such glass composites is evaluated by tests such as BS476 Part 22 or thermal shock method such as specified in ASTM E119, in both of which temperature of the unexposed surface is measured as a function of time. Since the aim of this work was to study the effect of fibre presence on intumescence, small sized samples (100 mm x 100 mm) were placed in a furnace and intumescence of the interlayer measured. Since both faces of the samples were exposed to heat, the thermal barrier effect of the intumesced samples could not be measured. The intumescence performance has been characterized in terms of degree of intumscence (DI) and density of the intumescent foam and the results are given in Table 5. The DI for PS-A and PS-B silicates in respective composite samples is 12.7 and 7.0, respectively. The higher degree of intumescence in PS-A compared to the PS-B silicate layer in these respective composites, illustrated by comparing Figures 1(b) and (c), is due to the higher amount of silica (see Table 1), and hence lower SiO_2 : Na_2O molar ratio (2.5:1) in the former. This observation also correlates

with the higher masses loss observed in TGA experiments in the temperature range 120-330 ^{o}C (see Table 4). On the other hand and due to the higher SiO_2 : Na_2O molar ratio in PS-B silicate (3.3:1), while the expansion of the silicaceous char is less (see Figure 1(c)), it is more rigid and compact compared to that for the PS-A silicate in Figure 1(b). This increased compactness is also evident from the higher foam density of PS-B (210 kg/m^3) compared to that for PS-A (140 kg/m^3) as seen from Table 5. The compact, intumescent, silicaceous char layer of PS-B, however, is reported to be more thermally stable with low thermal conductivity and can reduce heat and oxygen transmission and render better fire retardancy [7, 20] than less compacted PS-A silicate intumescent layers.

For PP and PA66 web-reinforced, PS-A silicate, composite samples the DI values are 10.5 and 10.3 respectively, which are lower than that of the PS-A composite sample. For ARGV nonwoven veil and steel mesh-reinforced, PS-A silicate samples, the DI values are also lower (10.8) than the PS-A sample (see Table 5). On the other hand, for ARGM woven mesh reinforced PS-A silicate, there is a minimal effect of the reinforcement on DI in that DI = 12.3 for the PS-A+ARGM and 12.7 for the PS-A composite. A similar trend is observed for the foam densities of fibre-reinforced, PS-A composite samples. For the PS-A+ARGM composite, the foam density is similar to that of the PS-A sample without fibre (140kg/m^3) but for other fibre-reinforced PS-A composite samples, this value is slightly higher (145-155kg/m^3) (see Table 5) indicating that the intumescent, silicaceuos char is more compact due to fibre reinforcement.

The total amount of silicate varies in the different composite samples due to presence of different amounts of fibres as nonwoven or mesh structures as shown in Table 2. To establish whether

there is a relationship between fibre concentration (independent of fibre type) and reduction in DI, the fibre content in each composite sample (Table 2) versus the percent differential DI value, $\Delta DI(\%) = ((DI_{(PS\text{-}A/B+fibre)} - DI_{PS\text{-}A/B}) / DI_{PS\text{-}A/B}))*100$ is plotted in Figure 4(a), where PS-A/B denotes that either respective PS-A or PS-B sample data were used. Although the data is somewhat scattered, there appears to be a general negative inverse relationship between $\Delta DI(\%)$ values and fibre content. Thus it would appear that both PP and PA66 fibres present in web form having the lowest mass percentages reduce DI the most with respect to the PS-A composite, while the PS-A+ARGV composite with a higher mass percentage promotes a lower DI reduction. Thus, as can be seen from Tables 2 and 4 and Figure 4(a), the presence of ARGM as a woven mesh at about twice the percentage by mass of ARGV has minimal effect on the DI of the silicate. The negative inverse $\Delta DI(\%)$ versus fibre mass percentage trend indicates that the structure of the reinforcement and fibre type are possible dominant factors in this case. Filament diameters are listed in Table 2 for each of the reinforcing structures and if these were to exert a significant effect on DI values, it might be expected that the ARG glass-containing reinforcements with lowest filament diameters would have a different effect to the steel mesh-containing composites containing the coarsest filaments. Figure 4(a) shows no such effect with composites containing steel and ARGV reinforcements having similar DI values. Previously published images of the reinforcing fabrics used (see Figure 1, reference 15) shows that the nonwoven structures comprise random arrays of individual filaments whereas the woven meshes, particularly ARGM, is a very open grid-like structure which would offer much less resistance to a molten matrix undergoing intumescence. Moreover, the thermoplastic fibres present melt and the molten polymer will affect the rheology of the silicate while it is intumescing unlike the inert glass or steel filaments. To attempt to shed further light on this interesting trend, the possible

correlation of DI values in composites with water release in the temperature range 40-330^{o}C from TGA curves of respective, equivalent silicate/fibre mixtures was investigated. The mass loss up to 330^{o}C of each sample mixture was calculated by averaging the mass loss relating to respective silicate content and fibre content in Table 2, using the values for mass loss for each silicate sample and fibre from Table 4. Differential mass loss values in the temperature range 40-330 ^{o}C, $\Delta m = m_{(PS\text{-}A\ +\ fibre)} - m_{PS\text{-}A}$ where (PS-A+fibre) and (PS-A) subscripts are the respective masses, were calculated and plotted against percent differential DI values, Δ DI(%), defined above (see Figure 4(b)). These results also show that while fibre type has some effect, notably any tendency to melt, the dominant factor appears to be the reinforcement fabric structure which affects the intumescence.

In case of PS-B silicate composite samples the presence of PP and PA66 fibre webs reduce the DI of PS-B from 7.0 to 6.7. ARGV and the steel fibre mesh also marginally reduce the value to 6.7-6.9. The ARGM woven mesh (PS-B+ARGM) composite though has no noticeable effect on DI (Table 5).

As seen from Figure 4(a), the percentage reduction in DI for each PS-B sample is less than that of the respective PS-A sample containing the same fibre reinforcement. A similar trend is observed for foam density values which increase with fibre presence, except for the ARGM-containing sample (PS-B+ARGM) where the foam density remains unaffected at 212 kg/m^3(see Table 5).

Figure 4(b) contains the analogous Δm versus ΔDI(%) data for the PS-B composites as was undertaken for the PS-A composite samples above and here, once again, the same trend is observed. Thus again, as the TGA-derived, differential mass loss of water decreases from silicate/fibre mixtures as fibre content increases so an almost negative linear ΔDI(%) versus Δm trend is observed.

In conclusion, therefore, from the thermal shock test results, it can be observed that the presence of both PP and PA66 fibres reduce the intumescence properties of both PS-A and PS-B silicates even at their low mass percentage levels. This effect was more pronounced, when observed during the thermal analysis of their mixtures, which may be due to the more uniform mixing of fibres with silicate powder compared with the composite analogue sample. Also the longer heating times experienced compared to the thermal shock experiments will allow fibres to melt and decompose more thoroughly. In thermal shock testing, while the composite samples were subjected to 450 ^{o}C for 5 minutes, it is expected that fibres would be partially melted/decomposed. This statement is supported by the observation in thermally shocked composites of partially melted/decomposed fibres as the SEM images of foamed samples in Figure 5(b) and 5(c) show. This partial decomposition of fibres, may also physically reduce the expansion of the intumescent silicate matrix, resulting in the observed slightly higher silicate-PP/PA66 layer densities shown in Table 5.

The reduced affects on the DI for ARG veil and ST mesh presence, as discussed above, is most likely a consequence of the glass fibres not melting and the difference between the veil and web fabric structures, with the latter being extremely open in character [15] and so offering less of a resistance to an intumescing fluid silicate matrix. The physical appearance of the intumescent

foam in the thermally-shocked, PS-A-ARGM sample is also similar to that of the sample without fibre as seen in Figures 5(a) and 5(d). Finally, it should be noted that, the organic polymeric fibrous compounds in the silicates can increase the flammability of the silicates by producing flammable degradation products [20,21] although this aspect is not examined in this study.

As mentioned earlier in this study the thermal barrier efficiency of these intumescent interlayers could not be determined due to small scale testing where uniform heat was applied to the samples in a furnace. In a future work large samples will be prepared and tested according to ASTM E110 and BS 476 part 22. However, based on our previous [14,15] and above results it can be envisaged that the fibre –reinforcement of silicates in commercially used glass-silicate-glass composites [5] will increase their impact resistance without adversely affecting the fire performance.

4. Conclusions

Thermal analytical results of silicate-fibre mixtures have indicated that the intumescent behaviour (determined as rate of release of water) of silicate matrices is affected in presence of synthetic fibres (PA66 and PP) as reinforcing elements in the matrices. However, an introduction of inorganic, thermally stable ARG glass fibres does not affect this behaviour of the matrices to the same extent and can increase the thermal stability of both silicate matrices compared to synthetic polymer fibres. The intumescence test results of the fibre-reinforced, silicate composites showed that all fibres in web/veil form affected the intumescence behaviour of both silicate interlayers although quite minimal. In fact, there was no observable effect of ARG woven mesh on the intumescence property of both silicates due to the open mesh structure of the

reinforcement and its ability not to impede the expansion of the intumescing matrix. This shows an open woven mesh of ARG fibres can be used as reinforcing elements within silicate matrices without significantly affecting the intumescent performance of the matrices. These types of composites have great potential to improve the impact resistance of commercially used fire-rated glass-silicate-glass composites such as those reported in Ref [5].

Acknowledgement

Authors would like to acknowledge Pilkington plc to sponsor this project and also for their financial support.

References

1. Razwick J. (1999) The next thousand years fire-rated glazing in the next millennium. *U.S. Glass.* **34 (6)**: 1-3.
2. Brinkmann N. (2000) Generating explosively hot ideas in fire-rated glazing. *U.S. Glass*. **35 (4)**:1-5.
3. Prewo KM, Brennan JJ, Layden K. (1986) Fibre reinforced glasses and glass ceramics for high performance applications. *Ceram. Bull.* **65**:305-22.
4. Bulewicz EM, Pelc A, Kozlowski R, Miciukiewicz A. (1985) Intumescent silicate-based materials: mechanism of swelling in contact with fire. *Fire Mater.* **9**:171-175.
5. Pilkington pyrostop®, Fire-resistant Glass Range, www.pilkington.com, 2013
6. Brough AR, Atkinson A. (2002) Sodium silicate based, alkali-activated slag mortars. *Cement and Concrete Research*. **32**:865-879.

7. Iler RK. (1979) The chemistry of silica: solubility polymerization, colloid and surface properties and bio-chemistry. Wiley-Inter -science, New York.
8. Langille KB, Nguyen D, Bernt JO, Veinot DE, Murthy MK. (1991) Mechanism of dehydration and intumescence of soluble silicate, Part I: effect of silica to metal oxide molar ratio. *J. Mat. Science*, **26:**695-703.
9. Zhuravlev LT. (2000) The Surface Chemistry of Amorphous Silica: Zhuravlev model, colloids and surface. *Physicochemical and Engineering Aspects*, **173:**1-38.
10. Vigil G, Xu Z, Steinberg S, Israelachvili J. (1994) Interactions of silica surface. *J. Colloid and Interface Science*, **165:**367-385.
11. Langille KB, Nguyen D, Bernt JO, Veinot DE, Murthy MK. (1993) Constitution and properties of phosphosilicate coatings. *J. Mat. Sci.*, **28:**4183-4178.
12. Bulewicz EM, Pelc A, Kozlowski R, Miciukiewicz A. (1985) Intumescent silicate –based materials: mechanism of swelling in contact with fire. *Fire Mater.*, **9:** 171-175.
13. Donal IW. (1995) Preparation, properties and applications of glass and glass-ceramic matrix composites. *Key Eng. Materials.* **108-110**: 123-144.
14. Akonda MH, Kandola BK, Horrocks AR. (2012) Effect of alkali and ultraviolet aging on physical, thermal, and mechanical properties of fibers for potential use as reinforcing elements in glass/silicate composites. *Poly. For Adv. Mat.*, **23 (11):**1454-1463.
15. Akonda MH, Kandola BK, Horrocks AR. (2014) The effect of fibrous reinforcement on optical and impact performance of fibre-reinforced transparent glass composites. *J. Mater. Sci*., **49**(**4**):1903-1913.
16. Pelegris C, Rivenet M, Traisnel M. (2005) Intumescent silicate: synthesis, characterization and fire protective effect. Chapter Five in fire retardancy of polymers-new applications of mineral

fillers", Eds. by Bras ML, Wilkie CA, Bourbigot S, Duquesne S. and Jama C. pub. RSC, Cambridge, UK.

17. McDonald RS. (1958) Surface functionality of amorphous silica by infrared spectroscopy. *J. Phys. Chem*., **62** (**10**):1168-1178.
18. Metcalfe E, Kendrick D. (1997) Silicon based flame retardant; recent advancement. *Flame Retardant Polym. Mater*., **8** :129-135.
19. Ayadi A, Palpou M, Iratni A. (2005) The durability of alkali–resistant glass fibres in cement matrix. *J. Phys. IV Franch*, **123:**155-158, Translated in English by EDP Sciences, France.
20. Fayokun, R. (2005) Study of the thermal behaviours of intumescent silicate materials. Ph.D. Thesis, University of Greenwich, UK.
21. Andersson KR, Dent Glasser LS, Smith DN. (1982) Soluble silicates. *ACS Symp. Series,* **194**:115

Table and Figure Captions

Table 1. Silicate matrices and their compositions

Table 2. Composition of glass-silicate-glass composite laminates

Table 3. DTA and DTG peaks maxima of dry silicates-fibre (5 and 10% fibre) mixtures .

Table 4. TGA actual mass losses and those calculated from component ratios (italicized in brackets) for PS-A and PS-B samples with 5 and 10% fibre content in the temperature range 100-350^{o}C

Table 5. Degree of intumescence and density of intumescent layer of silicate matrix in glass-silicate-glass composites

Figure 1. (a) Glass-silicate-glass composites; expansion of silicate layers under thermal shock: (b) PS-A and (c) PS-B.

Figure 2. (a,d) DTA, (b,e) TGA and (c,f) DTG responses in nitrogen of PS-A (a-c) and PS-B (d-f) silicates with 5% PA 66, PP and ARG fibres.

Figure 3. a) TGA – DTG curves of PS-A and PS-B silicate samples in nitrogen; b) mass loss from TGA curves in the temperature range RT–330^{o}C.

Figure 4. Relationship between a) fibre content in silicate composite and ΔDI(%), the percent differential degree of intumescence (=($DI_{(PS\text{-}A/B+fibre)}$ − $DI_{PS\text{-}A/B}$) / ($DI_{PS\text{-}A/B}$)*100) and b) the differential mass loss, Δm (= (percent mass loss PS-A/B) – (percent mass loss PS-A/B-fibre mixture)), calculated from the TGA mass loss values between 40 and 330 ^{o}C of silicate/fibre mixtures (Table 4) for each sample given in Table 2, and Δ DI(%).

Figure 5. SEM images of intumescent foams of (a) PS-A silicate only and containing (b) PP nonwoven web, (c) PA66 nonwoven and (d) ARG woven mesh

Table 1. Silicate matrices and their compositions

Silicate Solutions	SiO_2 (%)	Na_2O (%)	SiO_2 : Na_2O (w/w)	Molar ratio	Solid content (%)	pH
PS-A	31.1	12.45	2.5 : 1	2.58 : 1	43.6	11.8
PS-B	28.4	8.60	3.3 : 1	3.41 : 1	37.0	13.6

Table 2. Composition of glass-silicate-glass composite laminates

Silicate types	Fibres	Types of reinforcement	Area density of web/mesh* (g/m^2)	Fibre diameter* (µm)	Sample identity	Fiber contents in silicate, ** mass-%
PS-A	No fibres	-	-		PS-A	0
	PP	Nonwoven web	16 ± 1.1	20.0± 0.1	PS-A+ PP	0.65± 0.03
	PA66	Nonwoven web	19 ± 1.2	19.7± 0.1	PS-A+PA	0.92± 0.03
	AR-glass	Veil	46 ± 0.7	12.4± 0.2	PS-A+ARGV	1.61± 0.02
		Mesh	88 ± 1.0		PS-A+ARGM	3.14± 0.03
	Steel	Mesh	40 ± 0.4	30.9± 0.2	PS-A+ ST	1.43± 0.01
PS-B	No fibres	-	-		PS-B	0.0
	PP	Nonwoven web	16 ± 1.1	20.0± 0.1	PS-B+PP	0.75± 0.03
	PA66	Nonwoven web	19 ± 1.2	19.7± 0.1	PS-B+PA	0.98± 0.02
	AR-glass	Veil	46 ± 0.7	12.4± 0.2	PS-B+ARGV	1.85± 0.02
		Mesh	88 ± 1.0		PS-B+ARGM	3.65± 0.03
	Steel	Mesh	40 ± 0.4	30.9± 0.2	PS-B+ST	1.65± 0.02

Note: *The values presented are averages of six readings along the length of the samples
** Average of three replicate samples

Table 3. DTA and DTG peaks maxima of dry silicates-fibre (5 and 10% fibre) mixtures .

Samples	DTA Peak maxima, (°C)	DTG Peak maxima, (°C)
Silicate matrices		
PS-A	100 (En), 146 (En), 352 (Ex), 590 (En)	104, 140, 361, 506
PS-B	66 (En), 352 (Ex)	104, 190, 362, 506
Fibres		
PP	163 (En), 461 (En)	460
PA66	261 (En), 430 (En)	448
ARG	-	-
PS-A + Fibres		
PS-A + 5,10% PP	100 (En), 146 (En), 352 (Ex), 462 (En), 583 (En)	104, 140, 361, 465, 506 (s)
PS-A + 5,10 % PA66	100 (En), 146 (En), 255 (En), 352 (Ex), 405 (En), 590 (En)	104, 140, 361, 408, 506
PS-A+ 5,10% ARG	100 (En), 146 (En), 352 (Ex), 583 (En)	104, 140, 361, 506
PS-B + Fibres		
PS-B+5, 10% PP	66 (En), 352 (Ex)	104, 190, 362, 506
PS-B+ 5, 10% PA66	66 (En), 255 (En), 352 (Ex), 400 (En)	104, 190, 362, 506
PS-B +5, 10% ARG	66 (En), 167 (En), 352 (Ex)	104, 190, 362, 512

Note: DTA and DTG peaks maxima are similar for PS-A and PS-B with 5 or 10% fibre content. The results are reproducible to ± 1 °C.

Table 4. TGA actual mass losses and those calculated from component ratios (italicized in brackets) for PS-A and PS-B samples with 5 and 10% fibre content in the temperature range 100-350ºC

Samples	TGA mass loss, % 40-120 ºC		TGA mass loss, % 120-330 ºC		TGA mass loss, % 330-600 ºC	
Silicate matrices						
PS-A	7.0		17.4		7.7	
PS-B	8.6		12.0		8.2	
Fibres						
PP	1.2		1.2		99.0	
PA66	1.2		1.0		93.0	
ARG	0		0		0	
PS-A + Fibres	**5% Fibre**	**10% Fibre**	**5% Fibre**	**10% Fibre**	**5% Fibre**	**10% Fibre**
PS-A + PP	8.0 *(6.7)*	7.4 *(6.4)*	13.9 *(16.6)*	14.4*(15.8)*	15.4 *(12.3)*	14.7 *(16.8)*
PS-A + PA66	7.9 *(6.7)*	7.0 *(6.4)*	14.6 *(16.6)*	15.4 *(15.8)*	11.9 *(11.9)*	13.4 *(16.2)*
PS-A+ ARG	7.4 *(7.7)*	7.5 *(6.3)*	14.8 *(16.5)*	13.6 *(15.7)*	7.1 *(6.5)*	7.0 *(6.9)*
PS-B + Fibres	**5% Fibre**	**10% Fibre**	**5% Fibre**	**10% Fibre**	**5% Fibre**	**10% Fibre**
PS-B+ PP	7.7 *(8.2)*	6.8 *(7.8)*	12.4 *(11.5)*	11.6 *(10.9)*	13.0 *(12.7)*	17.5 *(17.3)*
PS-B+ PA66	7.4 *(8.2)*	7.5 *(7.8)*	12.4 *(11.5)*	11.7 *(10.9)*	12.9 *(12.5)*	14.5 *(16.7)*
PS-B + ARG	7.9 *(7.9)*	7.6 *(7.7)*	11.9 *(11.4)*	11.6 *(10.8)*	8.0 *(7.8)*	7.7 *(7.4)*

Note: The results are reproducible to ± 1%.

Table 5. Degree of intumescence and density of intumescent layer of silicate matrix in glass-silicate-glass composites

Fibre reinforce-ment	Mass of interlayer (silicate + fibre) (g)	Initial interlayer thickness (T_1, mm)	Intumescent foam thickness after test (T_2, mm)	Degree of intumescence (DI)	Foam density (kg/m^3)
PS-A	28.0 ± 0.2	1.5± 0.2	20.5± 0.2	12.7± 0.2	140± 1.2
PS-A+ PP	27.5± 0.8	1.6± 0.6	18.4± 0.8	10.5± 0.3	155± 1.8
PS-A+ PA66	27.5± 0.9	1.6± 0.6	18.0± 0.7	10.3± 0.3	153± 1.8
PS-A+ARGV	27.2± 0.7	1.5± 0.5	17.7± 0.6	10.8± 0.4	150± 1.4
PS-A + ARGM	27.8± 0.9	1.5± 0.6	20.0± 0.6	12.3± 0.4	140± 1.8
PS-A + ST	27.6± 0.5	1.5± 0.4	17.7± 0.6	10.8± 0.3	150± 1.4
PS-B	24.0 ± 0.3	1.4± 0.1	11.2± 0.3	7.0± 0.2	210± 1.2
PS-B+ PP	24.3± 0.9	1.4± 0.6	10.8± 0.6	6.7± 0.3	220±1.4
PS-B+ PA66	24.3± 1.0	1.4± 0.5	10.8± 0.5	6.7± 0.3	220± 1.6
PS-B+ARGV	24± 0.8	1.4± 0.5	11.0± 0.5	6.9± 0.3	215±1.5
PS-B + ARGM	23.4± 0.6	1.4± 0.6	11.2± 0.6	7.0± 0.4	212±1.6
PS-B + ST	24.1± 0.5	1.4± 0.4	10.8± 0.5	6.7± 0.3	215±1.3

Note: The values presented are averages of three tests

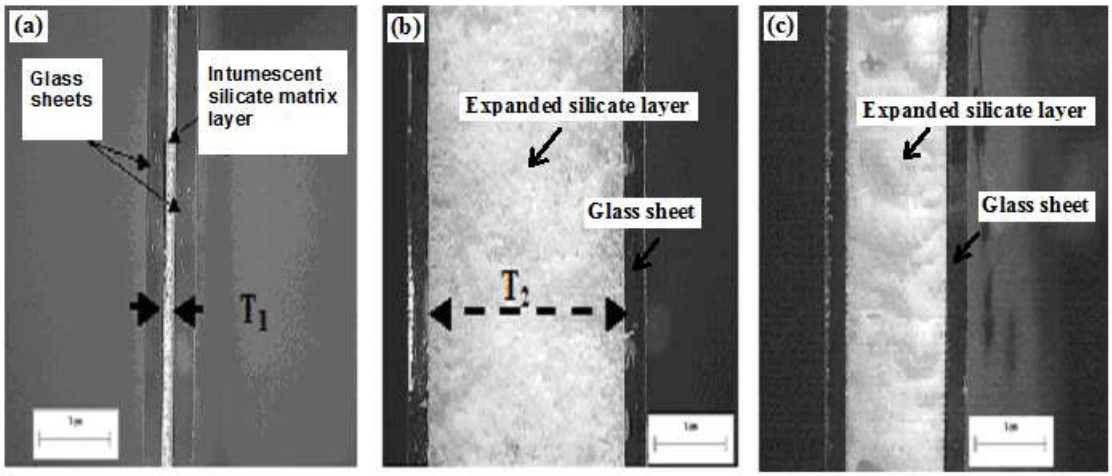

Figure 1. (a) Glass-silicate-glass composites; expansion of silicate layers under thermal shock: (b) PS-A and (c) PS-B.

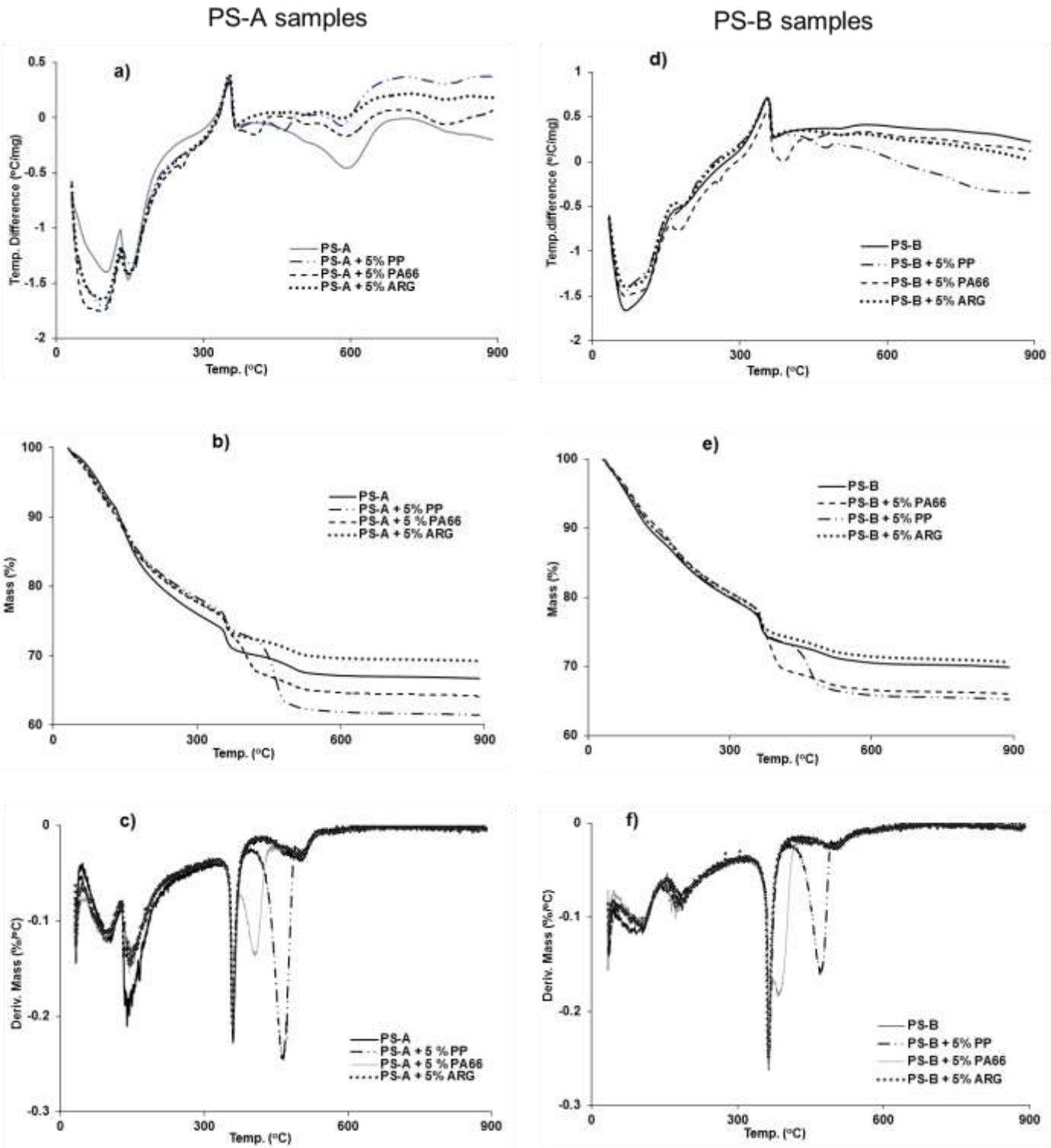

Figure 2. (a,d) DTA, (b,e) TGA and (c,f) DTG responses in nitrogen of PS-A (a-c) and PS-B (d-f) silicates with 5% PA 66, PP and ARG fibres.

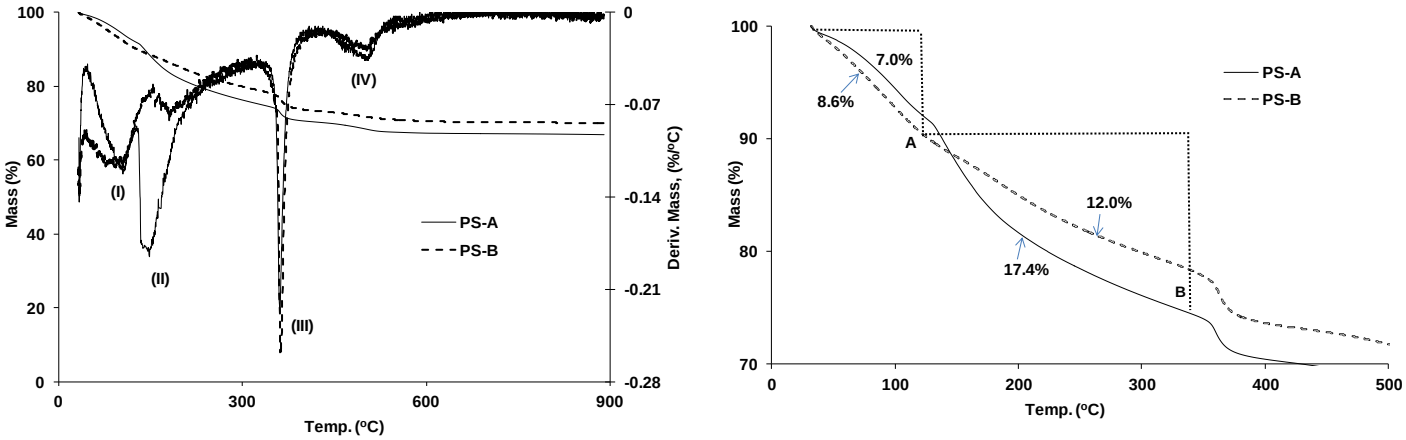

Figure 3. a) TGA – DTG curves of PS-A and PS-B silicate samples in nitrogen; b) mass loss from TGA curves in the temperature range RT–330ºC.

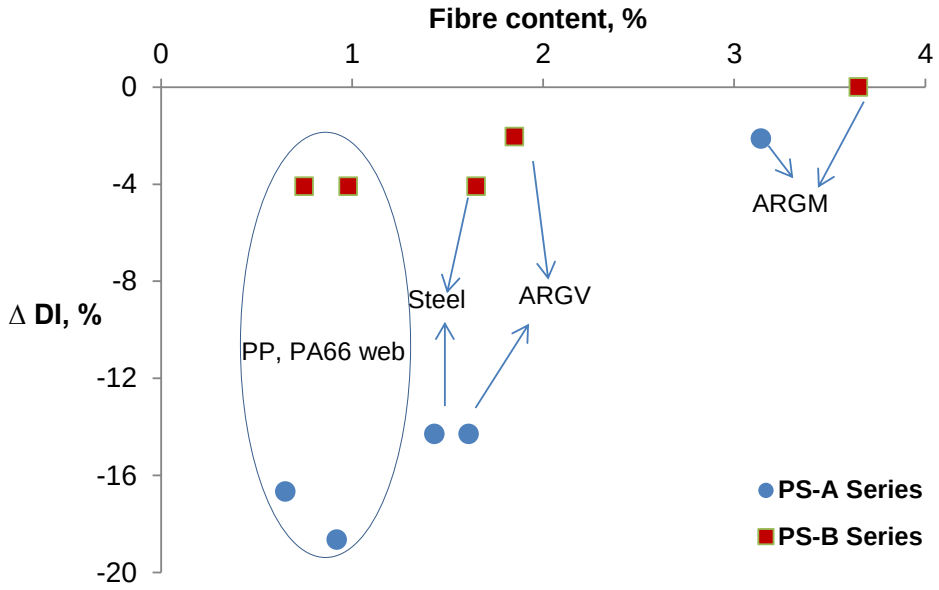

a)

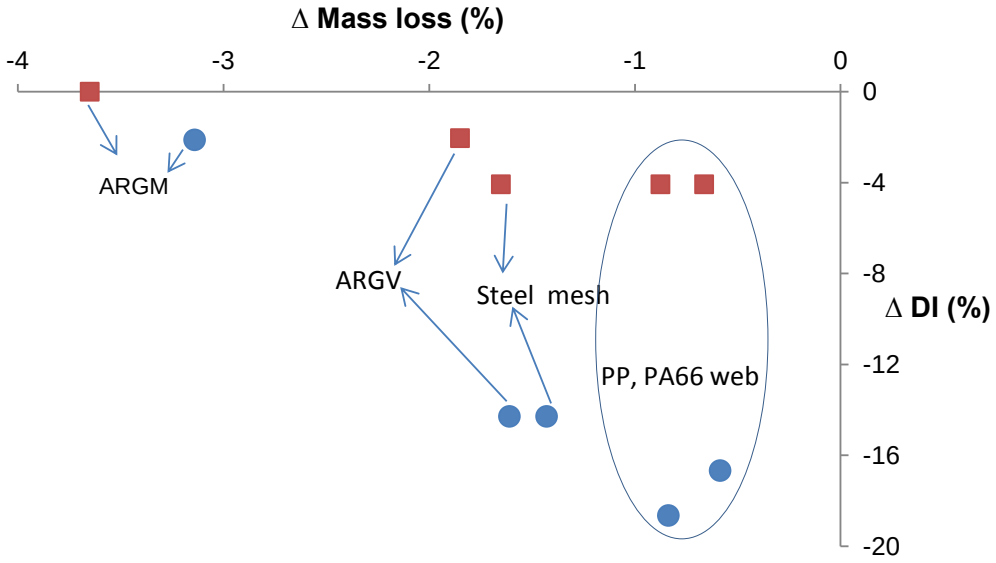

b)

Figure 4. Relationship between a) fibre content in silicate composite and ΔDI(%), the percent differential degree of intumescence (=($DI_{(PS\text{-}A/B+fibre)}$ – $DI_{PS\text{-}A/B}$) / ($DI_{PS\text{-}A/B}$)*100) and b) the differential mass loss, Δm (= (percent mass loss PS-A/B) – (percent mass loss PS-A/B-fibre mixture)), calculated from the TGA mass loss values between 40 and 330 ºC of silicate/fibre mixtures (Table 4) for each sample given in Table 2, and Δ DI(%).

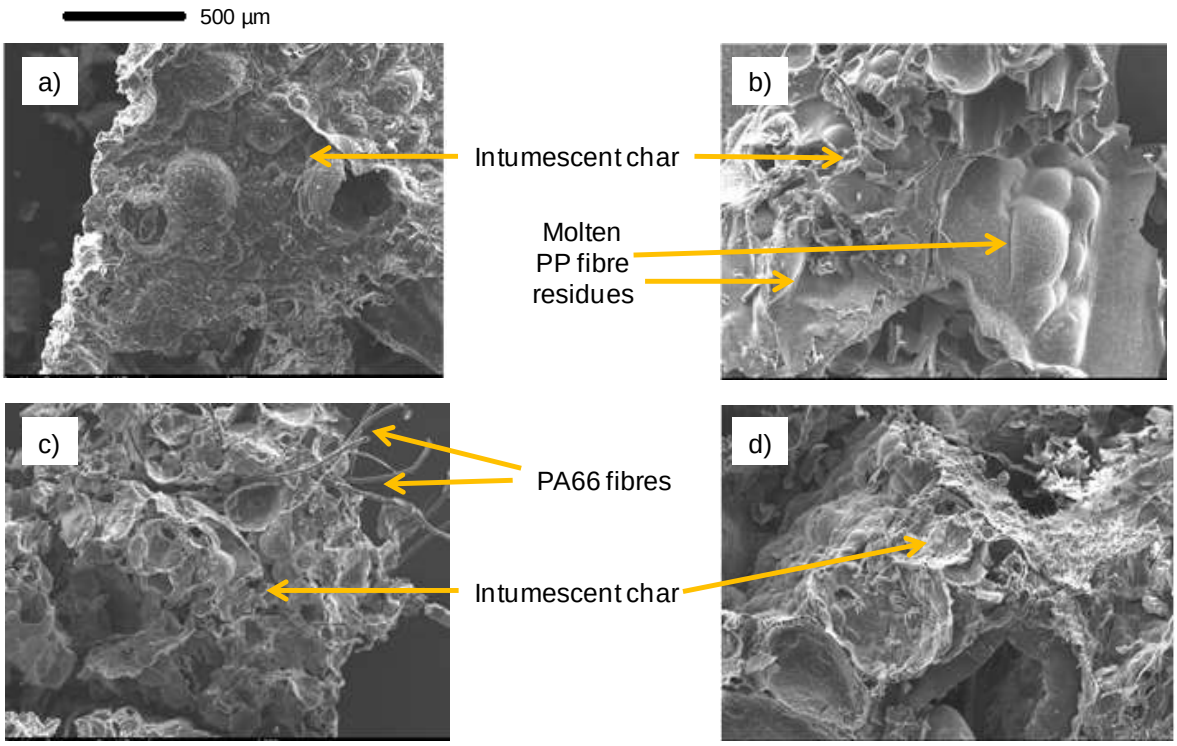

Figure 5. SEM images of intumescent foams of (a) PS-A silicate only and containing (b) PP nonwoven web, (c) PA66 nonwoven and (d) ARG woven mesh